CFD Assessment of the Inhaled Air Quality in a UFAD-Conditioned Office with Personalized Ventilation

Mohamad Kanaan
Mechanical Engineering Department, Faculty of Engineering, Beirut Arab University, Riad El Solh, Beirut, Lebanon
m.kanaan@bau.edu.lb (corresponding author)

Eddie Gazo-Hanna
College of Engineering and Technology, American University of the Middle East, Egaila, Kuwait
eddie-hanna@aum.edu.kw

Semaan Amine
College of Engineering and Technology, American University of the Middle East, Egaila, Kuwait
semaan.amine@aum.edu.kw

Received: 15 June 2025 | Revised: 31 July 2025 | Accepted: 11 August 2025

 DOI: https://doi.org/10.48084/etasr.12760

ABSTRACT

The quality of the inhaled air in an Underfloor Air Distribution (UFAD) system assisted by Personalized Ventilation (PV) is evaluated based on the CO_2 concentration levels in the respiration zone. Also, whole-body thermal comfort is assessed using the Predicted Mean Vote (PMV) model. A comprehensive three-dimensional Computational Fluid Dynamics (CFD) model is developed to simulate the indoor airflow behavior, including the interactions between the PV jet, human exhaled flow, and thermal plume. A parametric study is carried out by varying the UFAD and PV flow rates to analyze their effects on the overall thermal comfort and inhaled air quality. The results indicate that, for the proposed configuration and terminal device, PV with a supply temperature of 24 ºC and flow rates between 2.5 and 7.5 L/s may reduce the CO_2 concentrations in the respiration zone by up to 34%, while ensuring the occupant comfort. However, this finding cannot be generalized to all PV situations, as the present study accounts only for normal human breathing and a constant heat flux density. The variations in these parameters may alter the outcome due to the different interactions of the PV airflow in the occupant's microenvironment.

Keywords-underfloor air distribution; personalized ventilation; overall thermal comfort; inhaled air quality; CFD

I. INTRODUCTION

UFAD systems are widely regarded as energy-efficient air conditioning solutions that enhance the indoor air quality and thermal comfort [1, 2]. They are also reported to help reduce the airborne disease transmission in densely occupied environments. These systems deliver conditioned air through floor-mounted diffusers, which is then extracted by ceiling-mounted exhaust vents [3]. Unlike conventional mixing ventilation systems, UFAD permits supply air temperatures to be 4 – 7 °C higher [4], preventing occupant discomfort, particularly cold feet. This design leads to lower energy consumption by reducing the temperature difference across the cooling coil.

Moreover, the increased supply temperature strengthens the buoyancy-driven upward airflow, effectively transporting air contaminants to the upper part of the room and creating a stratified environment based on temperature [5]. The UFAD supply jet and the thermal plumes generated above the heat sources, play a crucial role in shaping the airflow dynamics within the conditioned space. A key design element in UFAD systems is the density interface level, which represents the height where the total thermal plume flow rate equals the supply air flow rate [6,7]. At this level, the space is separated into two distinct zones: a lower zone that remains cool and clean, and an upper zone that is warm and contaminated. To maintain good air quality in the occupied zone, the density interface must occur above the breathing level, as the exhaled contaminants tend to accumulate at this boundary, increasing exposure. This phenomenon, known as the lock-up effect, must be carefully managed to enhance the Quality of Inhaled Air (QIA) and mitigate the airborne disease transmission[8, 9].

Additionally, UFAD systems require the supply jet to have sufficiently high momentum flux to penetrate the density interface; otherwise, the system functions as displacement ventilation [10]. After reaching its maximum height, the supply jet reverses direction and falls back, leading to a mixing flow in the lower zone while the upper zone exhibits unidirectional airflow toward the exhaust vents [11, 12].

Reducing the supply flow rate has been shown to lower the density interface level, as the equilibrium between the supply air and thermal plume flow rates occurs at a lower height. While this can lead to thermal discomfort and unacceptable air quality in the occupied zone, it offers the economic benefit of reduced energy consumption.

This trade-off promotes the integration of PV, whose main idea is to provide cool and clean air in the vicinity of each occupant. PV systems customarily operate at low airflow rates and relatively high temperatures, making them a potential energy-efficient 'add-on' solution for maintaining thre comfort and air quality in UFAD systems with decreased ventilation rates.

Within the comfort range of room air temperatures (23–26°C), supplying PV air at 20°C enhances the air quality without inducing draught discomfort [13]. The PV impact on the indoor air quality in a displacement ventilation system was investigated by both analytical and CFD modeling [14]. The use of PV could improved QIA by 20% in the breathing zone. A transient CFD model was used to assess the performance of a personalized sinusoidal ventilation system in conjunction with mixing ventilation [15]. When operated at 22°C, with a flow rate of 7.5 L/s and a frequency of 0.94 Hz, the dynamic PV system provides the optimal balance between comfort and indoor air quality, achieving about 21% energy savings compared to constant PV. A PV system operating at a flow rate of 7–15 L/s can effectively lower the CO_2 concentrations in inhaled air while maintaining the occupant comfort in both mixing and displacement ventilation systems [16]. An experimental study assessed the role of PV in the airborne COVID-19 disease control [17]. Their findings suggest that PV can reduce the infection risk by up to 50%

The integration of PV with UFAD systems is largely unexplored in the literature [18]. Authors in [18] investigated the performance of UFAD assisted by PV in terms of the air quality, reporting that, at carefully selected flow rates, PV may improve the air quality in the occupant microenvironment by up to 25%. This paper aims to investigate, using CFD, the integration of PV with UFAD systems while assessing its impact on the air quality and overall thermal comfort. Unlike the limited number of existing UFAD–PV studies [18, 19], the present work first determines the UFAD flow rates required to ensure the thermal comfort. These optimized flow rates are then applied in PV integration scenarios, with the occupant comfort evaluated based on established criteria for the breathing zone and eye-level conditions. The proposed hybrid system is compared to a standalone UFAD system to ensure that both deliver the same QIA, while their respective energy costs are analyzed.

II. SYSTEM DESCRIPTION

The study considers a 2.5×2.5×2.6 m office in Beirut, containing a single workstation, as illustrated in Figure 1. The office features two external walls (north- and west-facing), two partition walls, and a ceiling and roof exposed to similarly conditioned spaces. The UFAD system serving the office includes two 20×20 cm supply diffusers and a 30 × 30 cm ceiling-mounted exhaust vent. The supply temperature is fixed at 20 °C.

The occupant is modeled as a block-shaped human simulator, positioned at a seated height of 1.25 m, with a total surface area of 1.72 m². It is assumed to emit 58.15 W/m² of heat (1 Met), corresponding to sedentary office work [20]. The circular mouth opening is taken to be 1.2 cm², representing average conditions for both breathing and talking [21]. The corresponding exhalation rate is 8.4 L/min [8], with the exhaled air containing 4% CO_2 at a temperature of 34°C. The PV terminal device, measuring 5 cm in diameter, is placed 40 cm in front of the occupant's face and supplies conditioned fresh air at 24°C, as depicted in Figure 2.

For simplicity, lighting fixtures are omitted from the geometry, and a lighting flux of 10 W/m² is applied to the ceiling assuming uniform distribution [22]. The office envelope follows a standard U-value of 1.6 W/m²·°C for buildings in Lebanon [23]. The external heat gains are estimated based on the outdoor design temperatures and the desired indoor temperature, which acts as the background temperature for PV. Although UFAD environments exhibit airflow stratification, leading to non-uniform indoor temperatures, using an average temperature would remain a reasonable approximation for the estimation of the external heat gains and thermal comfort assessment [24].

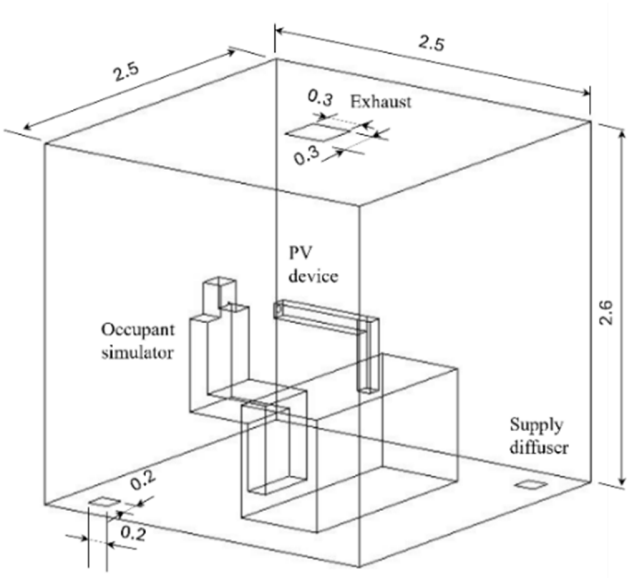

Fig. 1. Schematic layout of the office under study (dimensions in m).

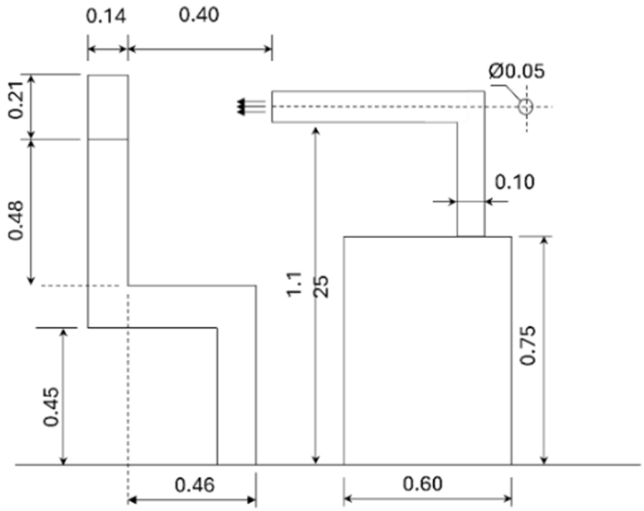

Fig. 2. Schematic layout of the PV configuration (dimensions in m).

III. CFD METHODS

CFD is a robust and accurate tool for analyzing the indoor airflow, particularly when appropriate models are selected and the boundary conditions are carefully defined [25, 26]. Other key factors contributing to a successful CFD simulation include the use of a high-quality computational mesh and ensuring a convergent, grid-independent solution.

A. Numerical Modeling

Using ANSYS Fluent, a detailed three-dimensional steady-state CFD model was developed to simulate the indoor airflow behavior and characteristics. To accurately solve the complex interactions between the occupant's thermal plume, exhaled airflow, and the PV jet, the careful selection of simulation models is essential. CFD predictions of temperature, velocity, and species concentration are then used to evaluate the overall thermal comfort and QIA in the UFAD space. The simulated geometry was discretized using the unstructured assembly method, ensuring mesh quality with a maximum skewness value below 0.9. Refinement with an element size of 5 mm was applied to the occupant's mouth, as well as the room's inlets and outlet, to accurately capture the high gradients in these regions. A grid independence analysis was conducted to evaluate the impact of the mesh size on the solution, as shown in Table I. The results led to the selection of Mesh 2 consisting of 676,492 elements, achieving a good balance between accuracy and computational efficiency.

TABLE I. RESULTS OF THE GRID INDEPENDENCE ANALYSIS

No. of cells		**Relative difference in predicted values of air properties at the exhaust with previous mesh value (%)**	
		Velocity	**Temperature**
Mesh 1	315,539	-	-
Mesh 2	676,492	17.2	6.2
Mesh 3	845,615	4.6	1.5

TABLE II. BOUNDARY CONDITIONS FOR THE SIMULATIONS

Boundary	**Type**	**Details**
Supply diffuser	Velocity inlet	Temperature = 20°C, Velocity = 0.3 – 0.7 m/s, CO_2 mole fraction = 0.0004, Turbulent intensity = 5%, Hydraulic diameter = 0.2 m.
PV inlet	Velocity inlet	Temperature = 24°C, Velocity = 1.27 – 3.82 m/s, CO_2 mole fraction = 0.0004, Turbulent intensity = 5%, Hydraulic diameter = 0.05 m.
Exhaust vent	Outflow	Flow rate weighting = 1
Person simulator	No slip	Heat flux = 58.15 W/m^2
Mouth	Velocity inlet	Temperature = 34°C, Velocity = 1 m/s, CO_2 mole fraction = 0.04 (4% in vol. of exhaled air), Turbulent intensity = 5%, Hydraulic diameter = 0.0133 m.
North-facing wall	No slip	Heat flux = 7.2 – 14.68 W/m^2
West-facing wall	No slip	Heat flux = 5.6 – 11.5 W/m^2
Ceiling	No slip	Lighting flux = 10 W/m^2
Wall partitions and floor	No slip	Zero heat flux

The Realizable k-epsilon model, incorporating enhanced wall treatment, with maximal y+ value of 0.82, was utilized to simulate the flow turbulence and accurately capture the viscous sublayer near walls, ensuring precise thermal plume predictions in the UFAD space [24]. For the simulations of UFAD with PV integration, the Standard k-omega model was employed to achieve higher accuracy and faster convergence. This turbulence model is better suited for simulating the air recirculation caused by localized vortices that may arise from the interaction of the two flows. To model buoyancy, which is critical in stratified environments with buoyancy-driven flows, the Boussinesq approximation was applied. The Surface-to-Surface (S2S) model was employed to account for the radiation effects. The velocity inlet boundary condition was used for both UFAD supply diffusers and PV inlet as the scalar air properties are known prior to the simulations [27]. The external wall heat fluxes were determined through energy simulations using DesignBuilder software and the design conditions of Beirut. The boundary conditions used in the simulations are detailed in Table II.

All variables, except pressure, were discretized using the second-order UPWIND scheme, while the STANDARD scheme was applied to the pressure term. To couple velocity and pressure in the Navier-Stokes equations, the SIMPLE algorithm was employed. Convergence was achieved when all scaled residuals reached 5×10^{-5}, the quantity of interest stabilized, and the net heat and mass fluxes became negligible.

B. Assessment of Thermal Comfort and Inhaled Air Quality

In the pre-processing phase of the simulations, a cuboid fluid zone was designated around the occupant to model its microclimate for thermal comfort evaluation. Volume-averaged air properties within this microclimate obtained from CFD were then used to evaluate the overall thermal comfort using the PMV model [28]. Personal factors, including the metabolic rate (1 Met for sedentary adult) and clothing insulation (0.6 clo $\equiv$0.093 m^2 °C/W), were incorporated into the PMV assessment

as well. The PMV scale ranges from -3 to +3, where -3 represents cold, -2 cool, -1 slightly cool, 0 neutral, +1 slightly warm, +2 warm, and +3 hot. The full details of the assessment methodology are found in our previous work [11]. The overall occupant comfort in the UFAD system is evaluated without PV integration. To ensure that the studied PV does not compromise the whole-body comfort established by the standalone UFAD system, its flow rate must remain below 7.5 L/s avoiding eye discomfort [15]. Additionally, an inhaled air temperature between 22 ºC and 30 ºC was proven to maintain comfort and prevent health issues [29]. Rigorously stated, since the PV flow specifically targets a localized area of the occupant, its use requires a segmental comfort analysis [30]. However, this aspect is beyond the scope of the current study.

To evaluate QIA, a 20 cm diameter sphere was created in front of the occupant's nose in the post-processing stage of the simulations, representing the respiration zone shown in Figure 3. Air quality is deemed acceptable when the volume-averaged CO_2 concentration in this zone remains below 1100 ppm, referencing an outdoor standard concentration of 400 ppm [31].

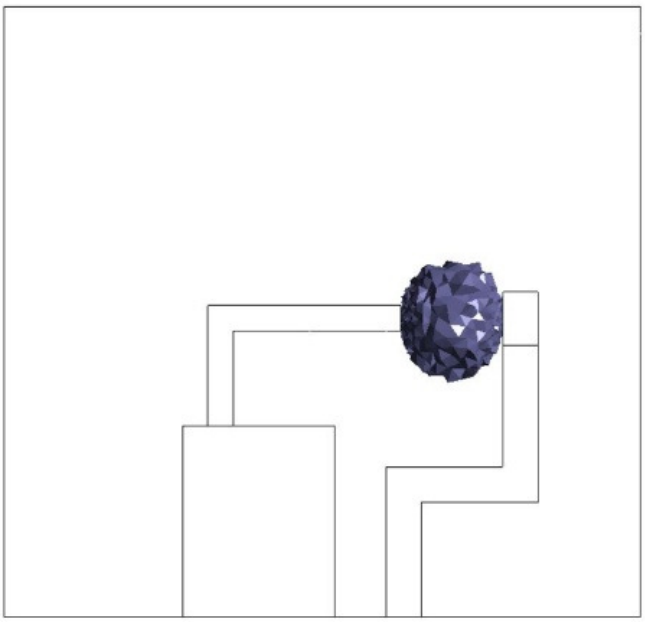

Fig. 3. Vector loops of the mechanism considered for synthesis.

C. Energy Analysis

The energy performance of the UFAD + PV system is evaluated by analyzing the total cooling coil load, considering the variations in the flow rates and temperature across both systems. The total cooling coil load is expressed in kW as:

$$Q = Q_{UFAD} + Q_{PV} = \dot{m}_{UFAD}(h_o - h_{s,UFAD}) + \dot{m}_{PV}(h_o - h_{s,PV}) \quad (1)$$

where $\dot{m}$ represents the supply flow rate in kg/s, and h_o and h_s denote the enthalpies of the outdoor air and supply air, respectively, expressed in kJ/kg. The outdoor summer design conditions for Beirut City, as specified in ASHRAE climatic design information [20], are 32.3°C (db) and 22.8°C (wb). The relative humidity of the supply air is approximated to that of the indoor design value of 44.6%. This assumption is valid since the conditioned office has negligible latent load compared to the room sensible loads.

D. Parametric Study

1) Simulations without PV Integration

The effect of the supply flow rate on QIA and thermal comfort in the specified UFAD space without PV integration is investigated through a CFD-based parametric study. In this stage, the focus is placed on understanding how the variations in the supply velocity influence both the distribution of fresh air and the perception of comfort in the occupied zone. The studied parameter range is chosen to align with the supply velocity values typically encountered in UFAD applications [6]. When the supply velocity falls below this range, the system's behavior resembles that of displacement ventilation, with stratified air layers forming in space. In contrast, when the velocity exceeds the upper limit of the range, the airflow pattern begins to resemble mixing ventilation, where stratification is weakened and uniformity dominates.

2) Simulations with PV Integration

For the simulations incorporating PV in comfort-compliant scenarios, QIA is evaluated at three distinct PV flow rates of 2.5, 5.0, and 7.5 L/s. These values were selected to represent a realistic operating range for PV, covering low, medium, and upper flow rate conditions. Across all cases, the PV supply temperature is maintained at 24 °C, while the outlet opening diameter remains fixed at 0.05 m, positioned 40 cm from the occupant's face to ensure consistent boundary conditions. This setup makes it easier to compare how different PV flow rates affect the quality of the inhaled air. Other factors, such as geometry and temperature, remain unchanged, so they do not interfere with the results. The supply temperature, outlet diameter, and PV-to-occupant distance are kept constant in all cases. This way, the effect of the flow rate can be seen more clearly. The parameter ranges used in these simulations are summarized in Table III.

TABLE III. RANGES OF STUDIED PARAMETERS

Parameter	Range
Standalone UFAD simulations	
Supply flow rate, (L/s)	Range A: 8, 12, 16, 20, 24, 28
(UFAD + PV) simulations	
UFAD flow rate, (L/s)	Range B: values of Range A resulting in whole-body comfort
PV flow rate (L/s)	2.5, 5.0, 7.5

IV. RESULTS AND DISCUSSION

A. Results without PV Integration

To examine how the UFAD supply flow rate affects the QIA and thermal comfort, six simulations were conducted for the considered office space without PV, with supply velocity varying from 0.3 m/s to 0.7 m/s, while the supply temperature remains unchanged. In each scenario, the predicted average air temperature and velocity within the occupant's microclimate,

along with the overall room temperature, were used to calculate PMV for thermal comfort assessment. Additionally, the predicted average CO_2 concentration in the inhaled zone served as a metric for evaluating QIA. The results are outlined in Table IV. The airflow velocity distribution on a cut plane passing through the supply diffuser, as well as along the symmetry plane, is presented for all simulated cases in Figure 4.

The contour plots illustrate that the UFAD supply jet throw gradually increases with supply velocity, with the strongest throw observed in case (e). This intensification shifts the density interface and makes the lock-up of exhaled contaminants more pronounced, particularly when the horizontal momentum of the exhaled airflow penetrates the thermal plume and disperses into the room. At higher flow rates, the thermal stratification is reduced and the thermal plume weakens. In case (d), this behavior results in a marked drop in the CO_2 concentration, as the density interface forms just above the occupant's nose and the exhaled airflow is directed upward into the head plume rather than spreading horizontally into the respiration zone. This outcome is linked to the strong vertical momentum of the convective UFAD flow, which counteracts horizontal exhalation and displaces CO_2 upward. In contrast, in case (e), QIA deteriorates again: the supply jet rises above the occupant's head before reversing and descending, thereby pushing exhaled air back into the respiration zone. The corresponding CO_2 concentration fields for all cases are presented on the symmetry plane in Figure 5.

Figure 6 displays the temperature contour plots inside the office, illustrating how the thermal stratification diminishes as the supply flow rate increases. In case (a), where the supply flow rate is the lowest, higher temperature levels are observed, leading to occupant discomfort due to a PMV value of 0.7, indicating a warm sensation. Conversely, in cases (d) and (e), the increased supply flow rate results in lower temperatures, causing the occupant to feel cold, with corresponding PMV values of -0.6 and -0.8, respectively.

TABLE IV. CFD PREDICTIONS OF AIR VARIABLES AND COMFORT METRICS FOR ALL STANDALONE UFAD CASE

Case	Supply flow rate (L/s)	Room temperature (°C)	Occupant's microclimate		PMV	CO_2 in respiration zone (ppm)
			Temperature (°C)	Velocity (m/s)		
(a)	12	28.03	29.87	0.051	0.7	1100
(b)	16	25.62	24.94	0.061	0	1048
(c)	20	24.33	24.01	0.078	-0.4	980
(d)	24	23.56	23.55	0.085	-0.6	511
(e)	8	23.13	23.15	0.093	-0.8	660

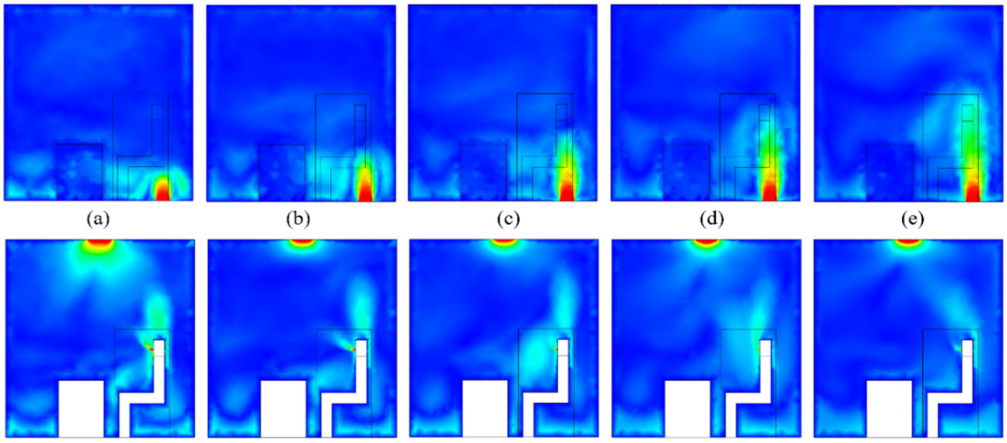

Fig. 4. Velocity contour plots on a cut plan through diffuser and a symmetry plane for standalone UFAD scenarios.

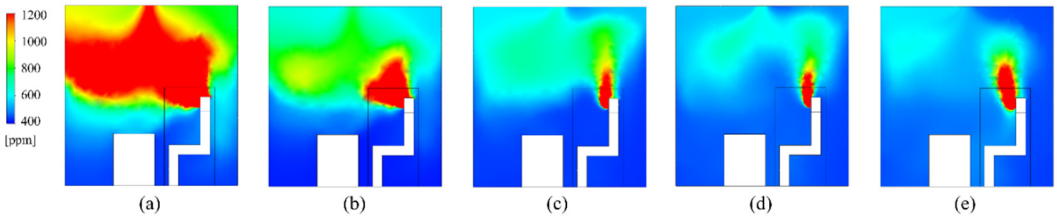

Fig. 5. CO_2 contour plots on the symmetry plane for standalone UFAD scenarios.

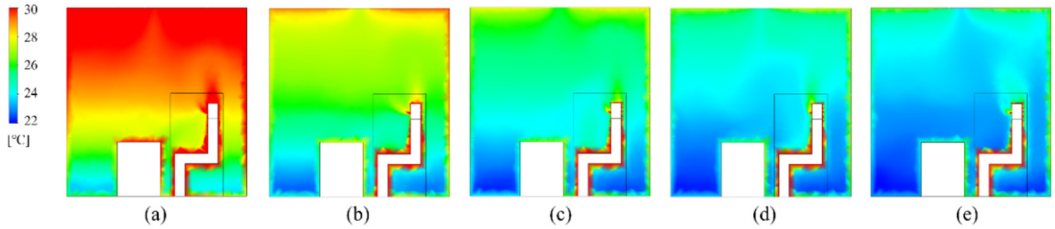

Fig. 6. Temperature contour plots on the symmetry plane for standalone UFAD scenarios.

TABLE V. PREDICTED QIA AND COMFORT METRICS FOR THE (UFAD + PV) SYSTEM

UFAD flow rate (L/s)	16			20		
PV flow rate (L/s)	2.5	5	7.5	2.5	5	7.5
Inhaled air temperature (°C)	30	29.6	29	28.1	27.7	27.4
CO_2 concentration (ppm)	801	757	695	766	731	664
QIA improvement (%)	24	27.8	34	22	25.4	32

B. Results with PV Integration

PV was integrated with UFAD in two comfort-compliant cases (b) and (c), with supply flow rates of 16 and 20 L/s, respectively. The office was then simulated using three different PV flow rates, 2.5, 5.0, and 7.5 L/s at a temperature of 24°C, with no adverse effect on the thermal comfort, as previously discussed. The results are portrayed in Table V.

The results indicate that the use of PV enhances QIA by up to 34% compared to UFAD, without compromising the overall comfort. In both UFAD scenarios, the inhaled air temperature remains between 22°C and 30°C, ensuring the thermal acceptability and perceived air quality [29]. The enhancement in QIA demonstrates that the PV diffuser sustains the minimum necessary flow rate, preventing the vortex formation within the respiration zone. However, when the velocity of exhaled airflow exceeds the current 1 m/s, momentum may override buoyancy, reducing the flow's deflection [9]. In such cases, the interactions between the PV airflow and exhaled breath create obstructions that trap the contaminants in front of the occupant's face, leading to poorer QIA [18].

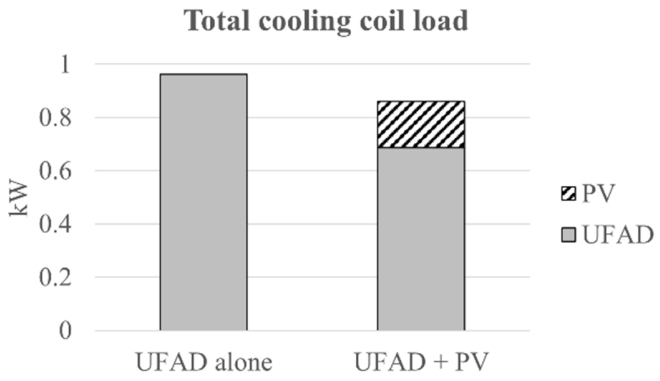

Fig. 7. Comparative plot of cooling coil load of UFAD alone in case (e) and UFAD + PV with the same QIA.

To investigate the potential energy savings, the cooling load will be compared between two cases, as shown in Figure 7: UFAD alone with a supply flow rate of 28 L/s, denoted as case (e) and a combined system with 20 L/s UFAD + 7.5 L/s PV. Both configurations maintain the same QIA level, with a CO_2 concentration of 660–664 ppm in the respiration zone. In this scenario, the UFAD + PV system achieves approximately 11% energy savings compared to the standalone UFAD system.

V. CONCLUSION

A three-dimensional CFD model was developed to evaluate the performance of a combined UFAD–PV system within a standard office environment. The analysis considered various UFAD and PV flow rates and examined their impact on both the overall thermal comfort and QIA. The whole-body comfort was assessed using the PMV model, while QIA was evaluated based the CO_2 concentration levels in the occupant's respiration zone.

The results demonstrate that PV is a viable solution for improving the inhaled air quality in UFAD spaces, particularly in situations where contaminants may become "locked up" at breathing height. In the studied cases, QIA in the respiration zone improved by 22–34% for PV flow rates ranging from 2.5 to 7.5 L/s. However, further research is needed to clarify the role of PV under a wider variety of exhaled flow rates, velocities, and human heat flux densities, as the complex interactions between the exhaled air, thermal plumes, and PV jets may alter the outcome. In some circumstances, these interactions may even reduce QIA.

From an energy perspective, the comparative analysis revealed that integrating PV with UFAD provides approximately 11% energy savings compared to standalone UFAD while maintaining the same level of inhaled air quality. Moreover, when appropriate control strategies are applied, PV integration may yield up to 55% energy savings compared to conventional air distribution systems [32, 33].

Although this study focuses on a small-scale office with a single workstation to optimize computational efficiency, the findings are relevant to other UFAD-equipped offices that share similar background flow characteristics and PV configurations.

REFERENCES

[1] S. A. Zolfaghari, A. Tavassolizade, S. Teymori, H. Keshavarz, and M. Raesi, "Experimental investigation of the effect of flow pattern in underfloor air distribution system on occupants' thermal comfort and energy consumption management," *2024 9th International Conference on Technology and Energy Management (ICTEM)*, IEEE, Feb. 2024, pp. 1–4, https://doi.org/10.1109/ICTEM60690.2024.10631978.

[2] K. Zhang, X. Zhang, S. Li, and X. Jin, "Review of underfloor air distribution technology," *Energy and Buildings*, vol. 85, pp. 180–186, Dec. 2014, https://doi.org/10.1016/j.enbuild.2014.09.011.

[3] C. H. Cheong, B. Park, and S. R. Ryu, "Effect of under-floor air distribution system to prevent the spread of airborne pathogens in classrooms," *Case Studies in Thermal Engineering*, vol. 28, Dec. 2021, Art. no. 101641, https://doi.org/10.1016/j.csite.2021.101641.

[4] A. Alajmi and W. El-Amer, "Saving energy by using underfloor-air-distribution (UFAD) system in commercial buildings," *Energy Conversion and Management*, vol. 51, no. 8, pp. 1637–1642, Aug. 2010, https://doi.org/10.1016/j.enconman.2009.12.040.

[5] Q. Kong and B. Yu, "Numerical study on temperature stratification in a room with underfloor air distribution system," *Energy and Buildings*, vol. 40, no. 4, pp. 495–502, Jan. 2008, https://doi.org/10.1016/j.enbuild.2007.04.008.

[6] M. Kanaan, "Modelling of contaminant dispersion in underfloor air distribution systems: comparison of analytical and CFD methods," *Journal of Building Performance Simulation*, vol. 12, no. 6, pp. 759–769, Nov. 2019, https://doi.org/10.1080/19401493.2019.1655096.

[7] S. Schiavon, K. Lee, F. Bauman, and T. Webster, "Development of a simplified cooling load design tool for underfloor air distribution (UFAD) systems," *Final Report to California Energy Commission Public Interest Energy Research Program*, Sacramento, CA, USA: California Energy Commission, 2010.

[8] N. Gao, J. Niu, and L. Morawska, "Distribution of respiratory droplets in enclosed environments under different air distribution methods," *Building Simulation*, vol. 1, no. 4, pp. 326–335, Dec. 2008, https://doi.org/10.1007/s12273-008-8328-0.

[9] F. Liu, L. Zhang, and H. Qian, "The penetration phenomenon of the expiratory airflow from thermal plume of human body in the microenvironment around people," *Building and Environment*, vol. 259, Jul. 2024, Art. no. 111656, https://doi.org/10.1016/j.buildenv.2024.111656.

[10] Y. J. P. Lin and P. F. Linden, "A model for an under floor air distribution system," *Energy and Buildings*, vol. 37, no. 4, pp. 399–409, Apr. 2005, https://doi.org/10.1016/j.enbuild.2004.07.011.

[11] M. Kanaan, S. Amine, and E. Gazo-Hanna, "Optimizing supply conditions and use of return air in UFAD system: Assessment of IAQ, thermal comfort and energy performance," *Results in Engineering*, vol. 24, Dec. 2024, Art. no. 103426, https://doi.org/10.1016/j.rineng.2024.103426.

[12] H. Ito and N. Nakahara, "Simplified calculation model of room air temperature profile in under-floor air-condition system," *International Symposium on Room Convection and Ventilation Effectiveness*, ASHRAE, 1993.

[13] J. Kaczmarczyk, A. Melikov, Z. Bolashikov, L. Nikolaev, and P. O. Fanger, "Thermal sensation and comfort with five different air terminal devices for personalized ventilation," *Roomvent*, Coimbra, Portugal, 2004.

[14] M. Kanaan, N. Ghaddar, and K. Ghali, "Quality of inhaled air in displacement ventilation systems assisted by personalized ventilation," *Heating, Ventilation, Air-Conditioning & Refrigeration Research*, vol. 18, May 2012, https://doi.org/10.1080/10789669.2012.649882.

[15] D. A. Assaad, K. Ghali, N. Ghaddar, and C. Habchi, "Mixing ventilation coupled with personalized sinusoidal ventilation: Optimal frequency and flow rate for acceptable air quality," *Energy and Buildings*, vol. 154, pp. 569–580, Nov. 2017, https://doi.org/10.1016/j.enbuild.2017.08.090.

[16] R. Cermak, A. Melikov, L. Forejt, and O. Kovar, "Performance of personalized ventilation in conjunction with mixing and displacement ventilation," *Heating, Ventilation, Air-Conditioning & Refrigeration Research*, vol. 12, pp. 295–311, Apr. 2006, https://doi.org/10.1080/10789669.2006.10391180.

[17] M. M. A. de Haas, M. G. L. C. Loomans, M. te Kulve, A. C. Boerstra, and H. S. M. Kort, "Effectiveness of personalized ventilation in reducing airborne infection risk for long-term care facilities," *International Journal of Ventilation*, vol. 22, no. 4, pp. 327–335, Oct. 2023, https://doi.org/10.1080/14733315.2023.2198781.

[18] B. Rahmati, A. Heidarian, and A. M. Jadidi, "The relation between airflow pattern and indoor air quality in a hybrid personalized ventilation with under-floor air distribution system," *Experimental Techniques*, vol. 47, no. 1, pp. 167–186, Feb. 2023, https://doi.org/10.1007/s40799-022-00595-0.

[19] Y. Li and P. V. Nielsen, "CFD and ventilation research," *Indoor Air*, vol. 21, no. 6, pp. 442–453, May. 2011, https://doi.org/10.1111/j.1600-0668.2011.00723.x.

[20] ASHRAE, *ASHRAE Handbook—Fundamentals, Chapter 14: Climatic Design Information*. Atlanta, GA, USA: American Society of Heating, Refrigerating and Air-Conditioning Engineers, Inc., 2021.

[21] J. K. Gupta, C.-H. Lin, and Q. Chen, "Characterizing exhaled airflow from breathing and talking," *Indoor Air*, vol. 20, no. 1, pp. 31–39, Feb. 2010, https://doi.org/10.1111/j.1600-0668.2009.00623.x.

[22] S. D. Ray, N.-W. Gong, L. R. Glicksman, and J. A. Paradiso, "Experimental characterization of full-scale naturally ventilated atrium and validation of CFD simulations," *Energy and Buildings*, vol. 69, pp. 285–291, Feb. 2014, https://doi.org/10.1016/j.enbuild.2013.11.018.

[23] P. H. Saleh, R. Schiano-Phan, and C. Gleeson, "A review of minimum U-values for Lebanon and the associated effect of internal gains," *33rd PLEA International Conference: Design to Thrive*, Edinburgh, UK, 2017.

[24] S. A. Nada, H. M. El-Batsh, H. F. Elattar, and N. M. Ali, "CFD investigation of airflow pattern, temperature distribution and thermal comfort of UFAD system for theater buildings applications," *Journal of Building Engineering*, vol. 6, pp. 274–300, Jun. 2016, https://doi.org/10.1016/j.jobe.2016.04.008.

[25] R. Mateus, A. Pinto, and J. M. C. Pereira, "Natural ventilation in large spaces: CFD simplified model validated with full-scale experimental data of Roman Baths," *Building and Environment*, vol. 266, Dec. 2024, Art. no. 112077, https://doi.org/10.1016/j.buildenv.2024.112077.

[26] M. Riaz *et al.*, "Experimental study of an air-conditioned tractor cabin using CFD analysis for primary and secondary tillage operations in Pakistan," *Results in Engineering*, vol. 26, Jun. 2025, Art. no. 104540, https://doi.org/10.1016/j.rineng.2025.104540.

[27] E. Alizadeh, A. Maleki, and A. Mohamadi, "An investigation of the effect of ventilation inlet and outlet arrangement on heat concentration in a ship engine room," Engineering, Technology & Applied Science Research, vol. 7, no. 5, pp. 1996–2004, Oct. 2017, https://doi.org/10.48084/etasr.1288.

[28] P. O. Fanger, Thermal Comfort, New York, NY, USA: McGraw-Hill, 1972.

[29] Z. Wu, N. Li, L. Lan, and P. Wargocki, "The effect of inhaled air temperature on thermal comfort, perceived air quality, acute health symptoms and physiological responses at two ambient temperatures," Indoor Air, vol. 32, no. 8, Aug. 2022, Art. no. e13092, https://doi.org/10.1111/ina.13092.

[30] R. Li, S. C. Sekhar, and A. K. Melikov, "Thermal comfort and indoor air quality in rooms with integrated personalized ventilation and under-floor air distribution systems," Heating, Ventilation, Air-Conditioning & Refrigeration Research, vol. 17, no. 5, pp. 829–846, Oct. 2011, https://doi.org/10.1080/10789669.2010.544834.

[31] Ventilation for Acceptable Indoor Air Quality, ASHRAE Standard 62.1, Atlanta, USA: American Society of Heating, Refrigerating and Air-Conditioning Engineers, 2016.

[32] D. A. Assaad, C. Habchi, K. Ghali, and N. Ghaddar, "Simplified model for thermal comfort, IAQ and energy savings in rooms conditioned by displacement ventilation aided with transient personalized ventilation," Energy Conversion and Management, vol. 162, pp. 203–217, Apr. 2018, https://doi.org/10.1016/j.enconman.2018.02.033.

[33] S. Schiavon, A. K. Melikov, and C. Sekhar, "Energy analysis of the personalized ventilation system in hot and humid climates," Energy and Buildings, vol. 42, no. 5, pp. 699–707, May 2010, https://doi.org/10.1016/j.enbuild.2009.11.009.